Design, Ion Beam Fabrication and Test of Integrated Optical Elements

I. Bányász[1], S. Pelli[2,3], G. Nunzi-Conti[2], G. C. Righini[3], S. Berneschi[2], E. Szilágyi[1], A. Németh[1], M. Fried[4,5], P. Petrik[4], E. Agócs[4], B. Kalas[4], Z. Zolnai[4], N. Q. Khanh[4], I. Rajta[6], G. U. L. Nagy[6], V. Havranek[7], V. Vosecek[7], M. Veres[8], L. Himics[8]

[1]*Department of Nuclear Materials Science, Wigner Research Centre for Physics, Hungarian Academy of Sciences, P.O.B. 49, H-1525, Budapest, Hungary*

[2]*MDF-Lab, "Nello Carrara" Institute of Applied Physics, IFAC-CNR, Via Madonna del Piano 10, 50019 Sesto Fiorentino (FI), Italy*

[3]*"Enrico Fermi" Center for Study and Research, Piazza del Viminale 2, 00184 Roma, Italy*

[4]*Research Institute for Technical Physics and Materials Science, Centre for Energy Research, Hungarian Academy of Sciences, Budapest, P.O.B. 49, H-1525, Hungary*

[5]*Institute of Microelectronics and Technology, Óbuda University, Tavaszmező u. 17, H-1084 Budapest, Hungary*

[6]*MTA Atomki, Institute for Nuclear Research, Hungarian Academy of Sciences, H-4001 Debrecen, P.O. Box 51, Hungary*

[7]*Nuclear Physics Institute AV CR, Řež near Prague, 250 68, Czech Republic*

[8]*Department of Applied and Nonlinear Optics, Wigner Research Centre for Physics, Hungarian Academy of Sciences, P.O.B. 49, H-1525, Budapest, Hungary*

Keywords: Ion Implantation, Integrated Optics, Optical Planar Waveguide, Optical Channel Waveguide, Optical Grating, M-Line Spectroscopy, Spectroscopic Ellipsometry, Micro Raman Spectroscopy, Rutherford Backscattering.

Abstract: Various methods, based on the use of ion beams, were used for the fabrication of planar and channel optical waveguides and Bragg gratings in optical crystals and glasses. Some examples of the results of these researches are presented in this review. Researches were initiated on ion beam fabrication of planar and channel optical waveguides in tellurite glasses. The ions used in the experiments were mainly helium, carbon, nitrogen and oxygen. In case of the two dimensional elements, like channel waveguides, both masked ion implantation and direct writing with ion microbeam were used. Optical microscopy (phase contrast, interference and interference contrast (INTERPHAKO), spectroscopic ellipsometry, m-line spectroscopy, Rutherford Backscattering and micro Raman spectroscopy were used to test the integrated optical elements.

1 INTRODUCTION

Realization of light confinement in optical guiding structures, both longitudinally and transversally, represented the milestone for the development of Integrated Optics (IO) devices of various functionalities, like optical amplification and light coupling or splitting, coexisting in a same chip (Miller, 1969 and Jaouen, 1999). Currently, the main effort in this field, coming from the research is that of discovering and developing the best materials – fabrication processes combination in order to reduce the cost and increase the performance of the previously mentioned devices. Glasses and crystals, because of their physical and optical properties, continue to find an even more increasing interest in different technology fields. Generally, glasses with their amorphous structure and relatively low refractive better interface with the optical fiber, thus resulting in lower values of coupling losses in the optical devices (Li, 2011 and Zou, 2001).

Glasses doped with Rare Earth (RE) ions are still the best choice for the development of integrated optical amplifiers where the request of a flat gain in a broader bandwidth is well satisfied by the disordered structure of these materials (Ogoshi, 2000 and Ohishi, 1998). Crystalline materials with their nonlinear properties and possibility of refractive index modulation by different effects, such as electro-optical and/or thermo – optical, are strongly used in different fields of the optoelectronics (Wooten, 2000 and Xu, 2015). Due to their ordered structure, these materials represent a suitable RE host for the

Bányász, I., Pelli, S., Nunzi-Conti, G., Righini, G., Berneschi, S., Szilágyi, E., Németh, A., Fried, M., Petrik, P., Agócs, E., Kalas, B., Zolnai, Z., Khanh, N., Rajta, I., Nagy, G., Havranek, V., Vosecek, V., Veres, M. and Himics, L.
Design, Ion Beam Fabrication and Test of Integrated Optical Elements .
DOI: 10.5220/0006679002790285
In *Proceedings of the 6th International Conference on Photonics, Optics and Laser Technology (PHOTOPTICS 2018)*, pages 279-285
ISBN: 978-989-758-286-8

realization of high gain and low threshold lasing devices (Sohler, 2005).

Ion beam irradiation, thanks to its high controllability and reproducibility, represents a suitable technique for the fabrication of integrated optical elements, such as active and passive waveguides and optical gratings, in most optical materials. (Townsend, 1994, Chen, 2007, Chen, 2012, Peña-Rodríguez, 2012).

Buried planar and channel waveguides were usually obtained using light ions (i.e.: protons, helium) via increasing the index of refraction of the target in a zone around the stopping range, which is relatively long for these kind of ions (Ren, 2010, Yao. 2011a, Yao, 2011b and Dong, 2011).

Medium-mass ions, especially carbon and oxygen, were also used for fabrication of optical waveguides in amorphous and crystalline materials (Tan, 2007, Zhao, 2010, Montanari, 2012, He, 2013, Liu, 2014).

Formation of adequate refractive index changes for waveguide fabrication with light and medium-mass ions requires relatively high fluences, in the 10^{15} -10^{17} ions/cm^2 region, especially when the mass and energy of the implanting ion are low.

The use of swift heavy ion irradiation for the modification of the optical properties of materials was first reported in the1990's. Aithal and his co-workers irradiated organic nonlinear optical crystals with 100 MeV Ag^{14+} ions, and studied optical properties of the irradiated samples (Aithal, 1997). Those results opened a new possible method of fabricating optical waveguides in the organic nonlinear optical crystals. Opferman et al. detected formation of amorphous tracks and layers in $KTiOPO_4$ crystals during implantation with swift heavy ions at low fluences (150 MeV Kr and 250 MeV Xe, $3\cdot10^{12}$ ions/cm^2 - $4\cdot 10^{13}$ ions/cm2) (Opfermann, 2000). Track and amorphous layer formation were due to electronic interaction, and could be explained using the Gibbons model (Gibbons, 1972). Olivares *et al.* reported on implantation of $LiNbO_3$ crystals using 5-MeV Si^{2+}, 7.5-MeV Si^{2+} and 30-MeV Si^{5+} ions with fluences from $5\cdot10^{13}$ ions/cm^2–$1\cdot10^{15}$ ions/cm^2 (Olivares, 2005a). They succeeded in producing optically isotropic amorphous layers of thicknesses increasing with the fluence. The same group succeeded in fabricating planar optical waveguides in $LiNbO_3$ crystals via implantation with 20 and 22 MeV fluorine ions and fluences from $1\cdot10^{14}$ ions/cm^2 - $3\cdot 10^{15}$ ions/cm^2 (Olivares 2005b). An amorphised layer situated around the maximum of electronic stopping power served as optical barriers while the layer left below the crystal surface remained crystalline and constituted the well of the optical waveguide.

2 EXPERIMENTAL

2.1 Planar Waveguides

Based on the results of our previous results of the fabrication of low grating-constant optical gratings in Pyrex glass with helium and nitrogen implantation in the 500 keV – 2 MeV energy range (Bányász, 2001), we opted for the use of nitrogen ions for the fabrication of planar optical waveguides. We succeeded in fabricating planar optical waveguides in an Er-doped tungsten-tellurite oxide glass with 1.5 MeV N^+ ion implantation at fluences up to 8 $\cdot10^{16}$ ion/cm^2 (Berneschi, 2011). The waveguides proved to operative up to the wavelength of 980 nm. This was due to the limitations caused by the small thickness of the guiding well, 1.6 µm, calculated by the SRIM code (Ziegler, 2004). Propagation losses in the waveguides were reduced by thermal annealing of the implanted samples. Further experiments using implantation with N^+ ions of an increased energy of 3.5 MeV resulted in planar optical waveguides in the same glass operating up the 1550 nm telecommunication wavelength (Bányász, 2012).

Appearance of the leaky modes in ion beam implanted planar optical waveguides is due to the low thickness of the barrier layer produced around the stopping range of the implanted ions. To overcome that problem, double-energy ion beam implantation was used (Bányász, 2013). Design of such planar waveguides is presented in **Figures 1 and 2.** The target material was sillenite type BGO crystal ($Bi_{12}GeO_{20}$). Double energy N^+ ion implantations were simulated using the SRIM code. The higher energy in each case was 3.5 MeV, the highest available energy at the one-

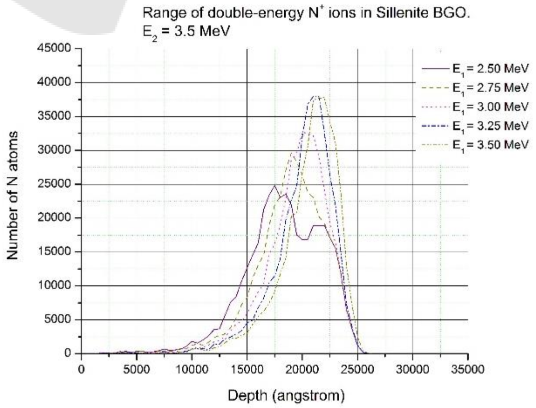

Figure 1: Depth-distributions of the implanted N^+ ions in sillenite type BGO crystal, calculated by the SRIM code. Higher energy was 3.5 MeV in each case. Lower energy is indicated in the inset.

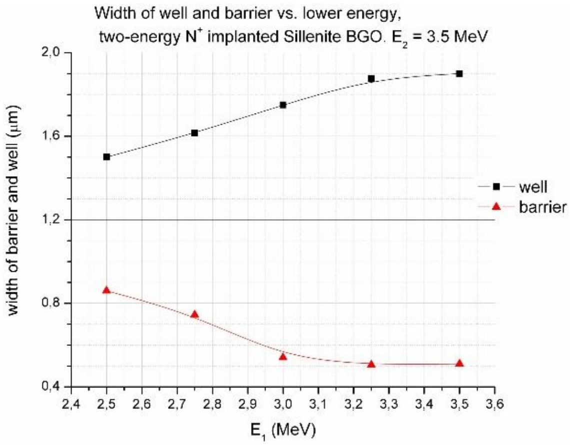

Figure 2: Width of the well and barrier layers *vs.* the lower energy of irradiation in the sillenite type BGO crystal.

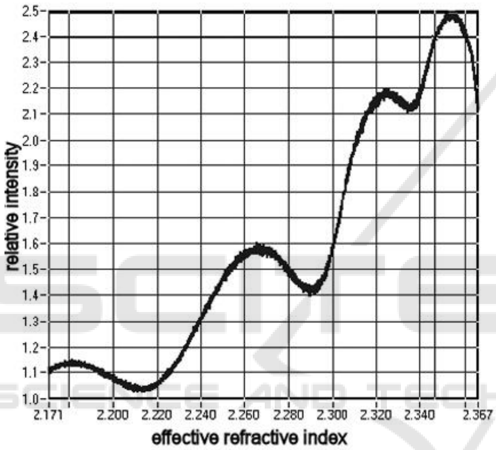

Figure 3: M-line spectra of the planar waveguide in sillenite type BGO crystal, irradiated with double energy N^+ ions at 3.5 MeV and 3.1 MeV, with a fluence of $2.0\cdot 101^{6}$ ions/cm^2, taken at 1310 nm.

stage accelerator used for those experiments, while the lower energies ranged from 2.5 to 3.25 MeV.

It can be seen in both **Figures 1** and **2** that higher implantation energy differences resulted in thicker barrier layers and slightly reduced well thickness. Waveguide operation at the 1310 and 1550 nm telecommunication wavelength was demonstrated in the planar waveguides fabricated in the Er-doped tungsten-tellurite oxide glass and the sillenite type BGO, see **Figure 3**.

With access to a modern Tandetron accelerator, implantation with higher-mass ions at higher energies became possible. In one of those experiments, planar optical waveguides were formed in an Er: $LiNbO_3$ crystal by implantation with 5 MeV N^{3+} ions. Calculated depth distribution of the ions in the target is shown in **Figure 4**.

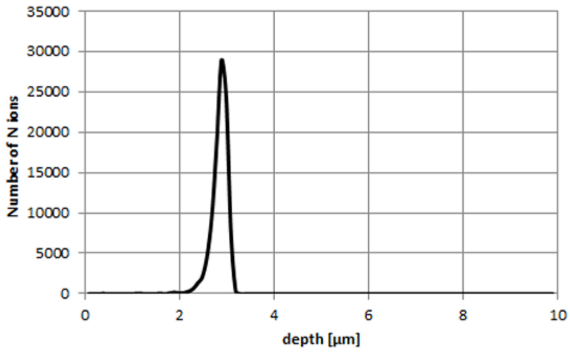

Figure 4: Depth distribution of 5 MeV N^{3+} ions in Er: $LiNbO_3$, calculated with SRIM.

The planar waveguides were studied by spectroscopic ellipsometry using a Woollam M-2000DI spectroscopic ellipsometer (wavelength range of 193-1690 nm). Reconstructed refractive index profiles of two of the waveguides are presented in **Figure 5.** Note difference in barrier position, width and height.

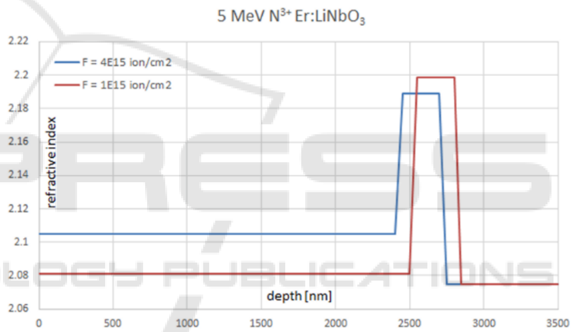

Figure 5: Fitted refractive index profiles of two ion-implanted planar waveguides. Er: LiNbO3 with 5 MeV N^{3+} ion at fluences of 1 and $4\cdot 10^{15}$ ion/cm^2.

2.2 Bragg Gratings

Multi-energy ion implantation makes it possible to fabricated optical elements structured in depth. Such elements can be stacked planar waveguides or Bragg gratings. Depth distribution of the implanted ions is of flat-topped skewed Gaussian, and the position of the peak of those curves changes monotonically with ion energy. Design of such a Bragg grating, made by the SRIM code, is shown in **Figure 6**. Total thickness of the Bragg grating was about 3 µm, grating constant Λ = 0.5 µm. However, depth distribution of the damage shows only about one third of the modulation seen in **Figure 6**.

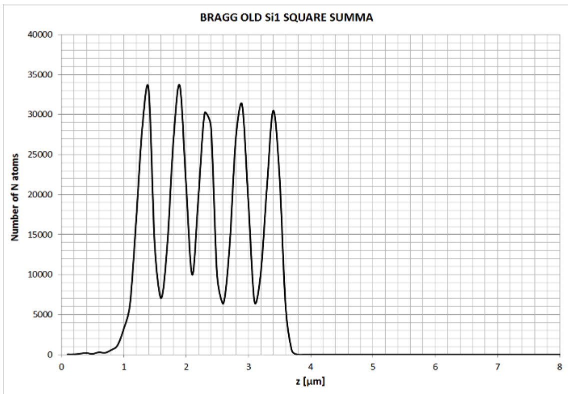

Figure 6: Calculated depth distribution of the implanted ions across a Bragg grating in silicon. The energies were 800 keV, 1.4, 2.0, 2.75 and 3.5 MeV.

The Bragg grating was studied using NIR reflectometry. The results of the measurement are presented in **Figure 7**. The high modulation in the reflectivity suggests a strong refractive index modulation in the grating.

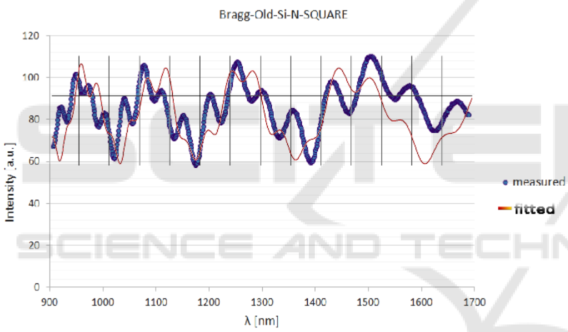

Figure 7: Measured (points) and fitted (red line) NIR reflectance of an ion-implanted Bragg grating. N^+, 800 keV $< E <$ 3.5 MeV, Si sample, Fluence per energy: $2 \cdot 10^{16}$ ion/cm^2.

Instead of varying the energy of the implanted ions in a bulk target, one can fabricate ion implanted Bragg grating in another way. One can combine the use of relatively low-energy ions and thin film deposition. Once a thin film of thickness corresponding to the designed grating constant of the Bragg grating is deposited on a substrate, it is implanted with low-energy ions of a suitable energy to obtain an ion distribution centered at the middle of the layer. Then the whole procedure is repeated until the desired total thickness of the Bragg grating is reached. Similarly, to the previous method, stacking of the ion-implanted thin layers can result in a quasi-sinusoidal depth profile of the refractive index.

Such Bragg gratings were prepared in SiO_2 thin films, both on silicon and glass substrates. The Bragg gratings were studied by Rutherford Backscattering Spectrometry (RBS). The results of the RBS study can be seen in **Figure 8**.

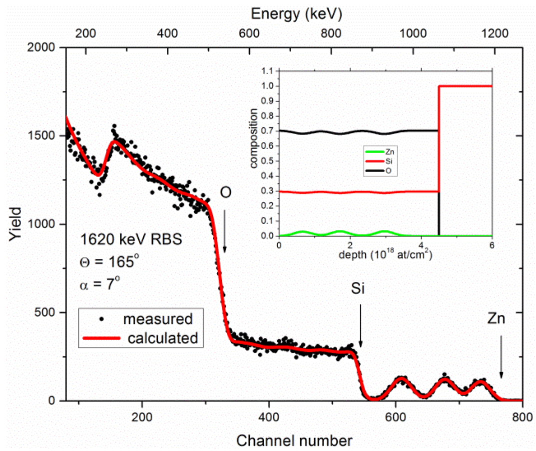

Figure 8: RBS measurement of an ion implanted Bragg grating.

The sample was prepared by repeating Chemical Vapor Deposition (CVD) of SiO_2 thin layers (first 300 nm and then twice 200 nm) and low-energy ion implantation of each layer by 130 keV Zn^+ ions on a silicon substrate. Both the measured and simulated RBS spectrum spectra and the calculated depth distribution (inset) of Zn in the sample show regular quasi-sinusoidal distributions. The high implanted fluences ($2 \cdot 10^{16}$ ions/cm^2 each) resulted in about 3 % peak Zn concentration (see inset). That concentration implies high modulation of the refractive index, so that even a low number of implanted grating layers could result in high diffraction efficiency.

Diffraction efficiency measurements of the various ion implanted Bragg gratings are under way.

2.3 Channel Waveguides

Two basic methods were used for the fabrication of channel waveguides in Er-Te glass, eulytine and sillenite type BGO crystals, CaF_2, $LiNbO_3$ and other optical crystals. The first one was implantation through masks. Various masks were used, such as a special silicon membrane mask that contained 24 µm wide slits and a patterned thick AZ4562 photoresist layer on the surface of the sample. The thickness of the channel waveguides was between 5 µm and 24 µm. Experiments using both methods were also carried out at the van de Graaff accelerator of the Wigner Research Centre for Physics, using N^+ ions at energies of 1.5 MeV and 3.5 MeV.

The second method was direct the writing of 15-µm channel waveguides in Er-Te glass with carbon, oxygen and nitrogen microbeams of low (around 5 MeV) and high (around 10 MeV) using a 3-MV Tandetron 4130 MC (High Voltage Engineering Europa B.V.) accelerator with a quadrupole triplet OM150 Oxford Microbeams Ltd. at the Řež Nuclear Physics Institute, Czech Republic.

Design of channel waveguides was similar to that of the planar ones. However, lateral confinement in the ion-implanted channel waveguides was not always automatically ensured in the experiments.

The first working channel waveguides were obtained in an Er: tungsten-tellurite glass, using a thick silicon membrane with 24 µm wide slits and implantation with 1.5 MeV energy N^+ ions (Berneschi, 2007). Guiding up to λ = 980 nm was demonstrated. Green upconversion at the same wavelength was also observed. Interference phase contrast (INTERPHAKO) microphotos of the channel waveguides are shown in **Figure 9**.

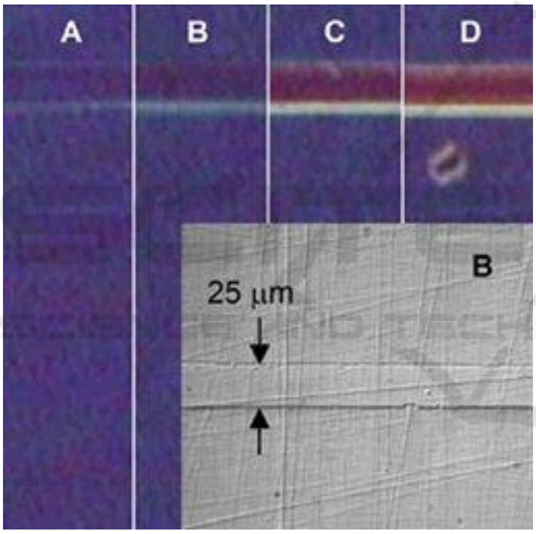

Figure 9: Interference phase contrast microscopic image of 1.5 MeV N^+ irradiated channel waveguides. Fluence was 0.5, 1, 2 and $4{\cdot}10^{16}$ /cm^2 for waveguides A, B, C and D. Inset: Conventional microscopic image of waveguide B.

In **Figure 9,** higher difference in hue corresponds to a higher difference in optical path, and hence refractive index modulation in the ion-implanted channel waveguides.

Profilometric scans (performed by a Talysurf device) of the ion implanted channel waveguides revealed that, depending on the implanted fluence, a swelling or depression of the implanted surface can occur. The results are shown in **Figures 10** and **11**.

Just a two-fold increase in fluence drastically changed the sign and profile of the surface change across the ion-implanted channel waveguide.

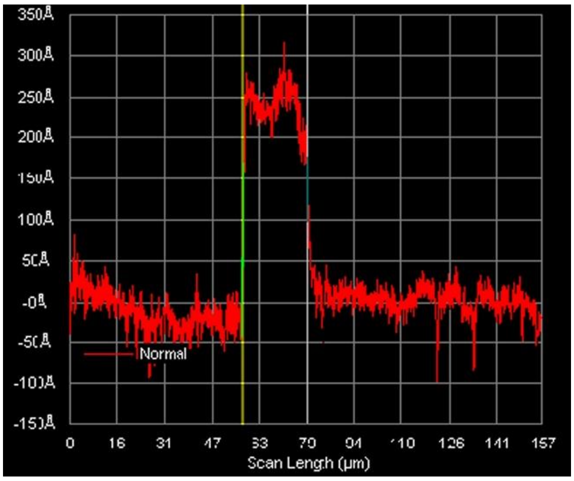

Figure 10: Profilometric scan across an ion implanted channel waveguide. Implantation: 1.5 MeV energy N^+ ions, fluence = $1{\cdot}10^{16}$ ions/cm^2. Rectangular ridge, h = 25 nm.

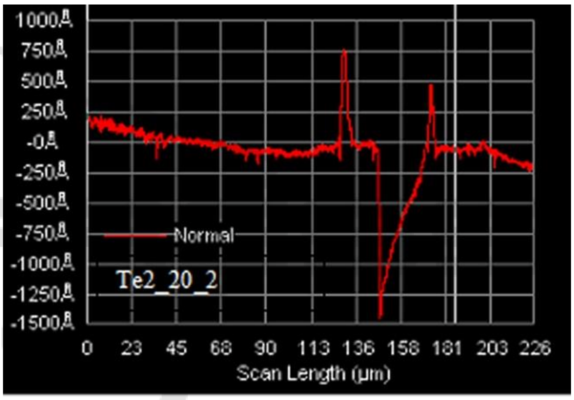

Figure 11: Profilometric scan across an ion implanted channel waveguide. Implantation: 1.5 MeV energy N^+ ions, fluence = $2{\cdot}10^{16}$ ions/cm^2. Triangular groove, h = 125 nm.

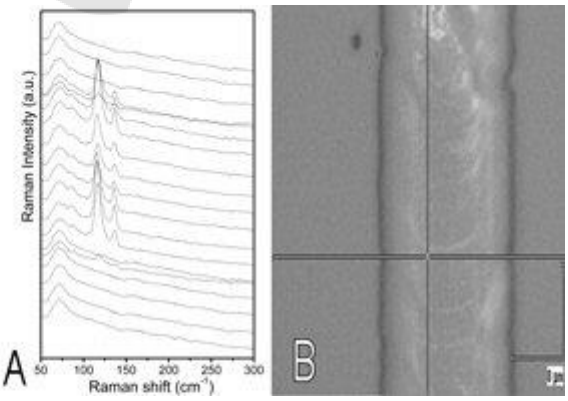

Figure 12: Micro Raman spectra (A) taken across a channel waveguide (B) fabricated in an Er-Te glass with 3.5 MeV N^{3+} ion irradiation through a silicon mask. Parameter of the curves is laser microbeam position along the horizontal line in the microphotograph.

More recently, the same method was used to fabricate channel waveguides in the same Er: tungsten-tellurite glass, but with N^+ ions of 3.5 MeV energy. Functionality tests of those channel waveguides are under way. The channel waveguides were also studied using micro Raman spectroscopy. Result of such a measurement is shown in **Figure 12**.

Note the appearance of new Raman lines in the implanted region, as very prominent manifestation of the structural changes caused in the target by the ion implantation.

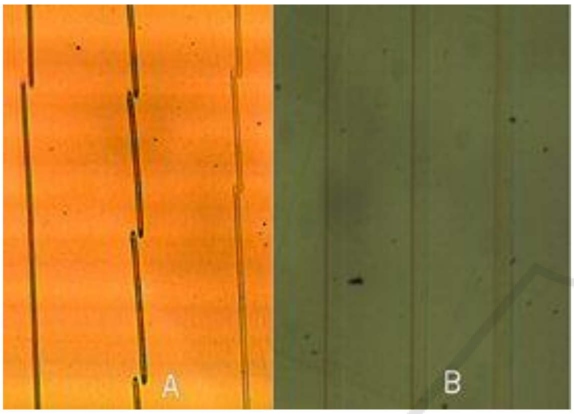

Figure 13: INTERPHAKO microphotographs of channel waveguides written in Er-Te glass with 6 MeV C^{3+} microbeam without charge compensation (A) and with an electron source (B).

As for the direct writing of channel waveguides, a number of samples have been completed so far, and functionality tests are under way. Just to illustrate the practical difficulties arising in such experiments, microscopic photographs of two sets of focused ion beam written channel waveguides are presented in **Figure 13**.

It can be seen that in the absence of charge compensation the electric field of the charge accumulating on the surface of the sample periodically deviates the ion microbeam, resulting in broken channel waveguides (**Figure 13** A). After installing an electron source in the vacuum chamber charge accumulation was eliminated, and contiguous channel waveguides could be written (**Figure 13** B).

3 CONCLUSION

It was proved that various integrated optical elements could be fabricated with ion implantation, using medium-mass ions, such as carbon, nitrogen and oxygen of energies in the 1–10 MeV range. Planar and channel optical waveguides and Bragg gratings were fabricated by the ion beam techniques. The optical elements were prepared in a number of optical crystals and glasses, e.g. sillenite and eulytine type BGO, doped and undoped $LiNbO_3$, SiO_2, Si and Er: -tungsten-tellurite glass. As for the results with ion implanted planar waveguides, it was found that nitrogen ion implantation resulted in higher refractive index contrasts and hence better confinement than the previously widely used proton and helium ion implantation. It proved to give even better results in several materials than carbon and oxygen implantation. Double-energy implantation was successfully adapted in those experiments to produce wider barriers and suppress leaky modes. Thermal annealing was used to eliminate or reduce lattice damages caused by the implantation and reduce propagation losses. Operation at telecommunication wavelengths of 1310 and 1550 nm was demonstrated in the waveguides written in the majority of the glass and crystalline materials studied. It was demonstrated that Bragg gratings of quasi-sinusoidal profile could be fabricated in glasses and crystals either by multi-energy implantation with MeV energy ions or by the combination of the growth of a stack of thin films and successive implantation of low-energy (50–100 keV) ions in each layer. In principle, high diffraction efficiency could be achieved with such gratings consisting of a relatively low number of grating periods, and having a moderate refractive index modulation. Ion beam implantation through special masks and direct writing with medium- to high-energy focused beams of medium-mass ions was proposed and used for the fabrication of channel waveguides. The first channel waveguides fabricated in an Er: -tungsten-tellurite glass by implantation through mask operated up to the wavelength of 980 nm. Although evaluation of a large part of the ion beam implanted optical elements is still under way, the results so far confirmed show that ion beam fabrication is an adequate method for fabrication of various types of optical elements. The use of swift heavy ions is an especially promising method, since it requires very low fluences (down to 10^{11} ions/cm^2), corresponding to short processing times.

ACKNOWLEDGEMENTS

This work was supported by the following funds: Hungarian National Research Fund, Project Number OTKA 115852. Part of this work has been carried out at the CANAM (Centre of Accelerators and Nuclear Analytical Methods) infrastructure LM 2015056. This publication was supported by the OP RDE, MEYS, and Czech Republic under the project CANAM OP, CZ.02.1.01/0.0/0.0/16_013/0001812.

REFERENCES

Aithal, P. Sreeramana, Nagaraja, H. S., Mohan Rao, P, Avasthi, D. K., and Sarma, Asati, *Journal of Applied Physics 81, 7526 (1997)*; doi: 10.1063/1.365294

Bányász, I., Fried, M., Dücső, Cs., and Vértesy, Z., *Appl. Phys. Lett., 79, 3755 (2001)*

Bányász, I., S. Berneschi, M. Bettinelli, M. Brenci, et al., "MeV energy N^+ - implanted planar optical waveguides in Er-doped tungsten-tellurite glass operating at 1.55 μm", *IEEE Photonics Journal, Volume 4, Issue 3, pp. 721-7, DOI: 10.1109/JPHOT.2012.2194997 (2012)*

Bányász, I., Z. Zolnai, M. Fried, T. Lohner, et al., "Single - and double energy N^+ ion irradiated planar optical waveguides in Er: Tungsten-Tellurite Oxide glass and sillenite type Bismuth Germanate crystals for telecom applications", Nuclear Instruments and Methods in *Physics Research Section B, 307, 299-304 (2013)*

Berneschi, S., G. Nunzi Conti, I. Bányász, et al., "Ion beam irradiated channel waveguides in Er^{3+}-doped tellurite glass", *Applied Physics Letters, 90, 121136, (2007)*

Berneschi, S, Brenci, M., Nunzi Conti, G., Pelli, S., et al., Slab optical waveguides in Er^{3+}-doped tellurite glass by N^+ ion implantation at 1.5 MeV, *Optical Engineering, 50, 071110 (2011).*

Chen, F., Wang, Xue-Lin and Wang, Ke-Ming, Opt. Mat., 29, 1523-1542, DOI: 10.1016/j.optmat.2006.08.001 (2007).

Dong, N., Jaque, D., Chen, F. and Lu, Q., "Second harmonic and Raman imaging of He^+ implanted KTiOPO4 waveguides", *Optics Express, 19, 13934-13939 (2011).*

Gibbons, J.F., Proceedings of the IEEE, 60, 1062 – 1096, (1972), DOI: 10.1109/PROC.1972.8854

He, Ruiyun, Shuqian Sun, Miaomiao Xu, Feng Chen, Shavkat Akhmadaliev, Shengqiang Zhou, Nucl. Instr. and Meth. in *Phys. Res. B, 308, 6-8 (2013)*

Li, S.- L. Han, P., Shi, M., Yao, Y., et al., "Low-loss channel optical waveguide fabrication in Nd^{3+}-doped silicate glasses by femtosecond laser direct writing", *Optics Express, 19, 23958-23964 (2011).*

Liu Chun-Xiao; Xu Jun; Xu Xiao-Li; Wu Shu; Wei Wei; Guo Hai-Tao; Li Wei-Nan; and Peng Bo, *Optical Engineering, 53(3), 037101 (2014)*

Jaouen, Y., du Mouza, L., Barbier, D. Delavaux, J., Bruno, P., "Eight-wavelength Er-Yb doped amplifier: combiner/splitter planar integrated module", *IEEE Photonics Technology Letters, 11, 1105 – 1107 (1999).*

Miller, S. E. "Integrated Optics: An introduction", *Bell System Technical Journal, 48, 2059 – 2069 (1969).*

Ogoshi, H., Ichino, S. and Kurotori, K., "Broadband Optical Amplifiers for DWDM Systems", Furukawa Review, No. 19, 17-21 (2000).

Ohishi, Y., Mori, A., Yamada, M., Ono, H., et al., "Gain characteristics of tellurite-based erbium-doped fiber amplifiers for 1.5 μm broadband amplification*", Optics Letters, 23, 274-276 (1998).*

Olivares, J., García, G., Agulló-López, F., Agulló-Rueda, F., Kling, A., Soares, J.C., Appl. Phys. A, 81, 1465–1469 (2005) DOI: 10.1007/s00339-005-3237-x

Olivares, J., García, García-Navarro, Agulló-López, F., A., Caballero, O., García-Cabañes, A, *Appl. Phys. Lett., 86, 183501 (2005)*

Opfermann, Th., Höche, Klaumünzer, S., Wesch, W, Nucl. Instr. and Meth. in *Phys. Res. B, 166-167, 954-958 (2000)*

Peña-Rodríguez, O., Olivares, J., Carrascosa, M., García-Cabañes, A., Rivera A. and Agulló-López, F., "Optical Waveguides Fabricated by Ion Implantations/Irradiation: A Review", in*: Ion Implantation, Prof. Mark Goorsky (Ed.),* ISBN: 978-953-51-0634-0, InTech, Available from: http://www.intechopen.com/books/ion-implantations/optical-waveguides-fabricated-by-ion-implantation-irradiation-a-review (2012)

Ren, Y., Tan, Y., Chen, F., Jaque, D., et al, "Optical channel waveguides in Nd: LGS laser crystals produced by proton implantation", *Optics Express, 18, 16258-16263 (2010).*

Sohler, W., Das, B., Dey, D., Reza, S., et al., "Erbium-Doped Lithium Niobate Waveguide Lasers", *IEICE Trans. Electron., E88-C, 990-997 (2005).*

Tan Y, Chen F, Physica Status Solidi-Rapid Research Letters 1 (6), 277-279 (2007)

Townsend, P. D., Chandler, P. J. and Zhang, L., Optical Effects of Ion Implantation, *Cambridge University Press, Cambridge, U.K. (1994)*

Xu, Kaikai, Liu, Haitao and Zhang, Zhengyuan, "Gate-controlled diode structure based electro-optical interfaces in standard silicon-CMOS integrated circuitry", *Applied Optics, 54, 6420-6424 (2015)*

Yao, Y., Tan, Y., Dong, N., Chen, F. and Bettiol, A. A., "Continuous wave Nd: YAG channel waveguide laser produced by focused proton beam writing", *Optics Express, 18, 24516-24521 (2011).*

Yao, Y., Dong, N., Chen, Vanga, S. K. and Bettiol, A. A., "Proton beam writing of Nd: GGG crystals as new waveguide laser sources", *Optics Letters, 36 4173-4175 (2011).*

Wooten, E. L. et al., "A Review of Lithium Niobate Modulators for Fiber-Optic Communications Systems", *IEEE Journal of Selected Topics in Quantum Electronics, 6, 69-82 (2000).*

Zhao, Jin-Hua, Liu, Xiu-Hong, Huang, Qing, Liu, Peng, Wang Lei and Wang, Xue-Lin, Nuclear Instruments and Methods in *Physics Research Section B: Beam Interactions with Materials and Atoms, 268, 2923–2925 (2010)*

Ziegler, J.F., "SRIM-2003", Nucl. Instr. and Meth.B, 219–220, 1027 (2004), and http://www.srim.org

Zou, J., Zhao, F. and Chen, R. T., "Two-step K^+-Na^+ and Ag^+-Na^+ ion-exchanged glass waveguides for C-band applications", *Applied Optics, 41, 7620-7626 (2002).*